Comparing Low and High-Temporal Resolution DCE-MRI Texture Analysis for Discrimination of Breast Lesions from Background Enhancement

Yufeng Liu
Zhejiang Chinese Medical University
Jiaying Li
Zhejiang Chinese Medical University
Jingjing Qu
Zhejiang Chinese Medical University
Rui Tang
Zhejiang University School of Medicine Second Affiliated Hospital
Kun Lv
Huashan Hospital Fudan University
Chundan Wang
Zhejiang Chinese Medical University
Fengchun Xiao
Zhejiang Chinese Medical University
Jiali Zhou
Ningbo First Hospital
Min Ge
Zhejiang Chinese Medical University
Xuewei Ding
Zhejiang Chinese Medical University
Hong Ding
Zhejiang Chinese Medical University
Shiwei Wang
Zhejiang Chinese Medical University
Maosheng Xu (xums166@zcmu.edu.cn)
The First Affiliated Hospital of Zhejiang Chinese Medical University; The First Clinical Medical College of Zhejiang Chinese Medical University https://orcid.org/0000-0002-2396-1600

Research article

Keywords: Breast, Magnetic resonance imaging, Dynamic contrast-enhanced, Texture analysis

Posted Date: December 22nd, 2020

DOI: https://doi.org/10.21203/rs.3.rs-132466/v1

Abstract

Background

Breast cancer is the most common cancer in women worldwide, high-resolution dynamic contrast-enhanced MRI (DCE-MRI) can better evaluate the tissue microenvironment and texture characteristics. The purpose of this study was to investigate the value of the texture-based analysis for breast DCE-MRI in the diagnosis of breast lesions and background enhancement.

Methods

This study prospectively enrolled 128 patients with clinically suspected breast lesions in our hospital from April 2015 to June 2017. Among them, 62 patients underwent preoperative high temporal resolution DCE-MRI (1 + 26 phases) scan with 39 malignant and 23 benign lesions. The control group retrospectively and randomly contained 78 patients who underwent preoperative low temporal resolution DCE-MRI (1 + 5 phases) scans with 46 malignant and 32 benign lesions. Quantitative parameters were obtained using a two-compartment Extended Tofts and volume of interest model for the lesion center, surrounding peripheral area and background enhancement, including pharmacokinetic parameters (K^{trans}, K_{ep}, V_e and V_p) and texture features based on the K^{trans} map. The Student's *t*-test was used to compare the differences of means. LASSO was used for dimension reduction and logistic regression analysis was used for model construction. A receiver operating characteristic (ROC) analysis was used to evaluate the diagnostic performance.

Results

Pharmacokinetic parameters were significantly different between high temporal resolution and low temporal resolution DCE-MRI ($P < 0.05$). In the malignant group, the average K^{trans} of the lesion area on high temporal resolution DCE-MRI was significantly correlated to the pathological grading ($r = 0.400$, $P = 0.012$). In the differentiation between benign and malignant lesions, the ROC analysis demonstrated that the diagnostic value of high temporal resolution DCE-MRI offered slightly significant advantages in the realms of the lesion, peripheral areas and background enhancement.

Conclusions

The use of texture analysis based on high temporal resolution DCE-MRI may potentially improve breast cancer diagnostic performance. Specifically, combining the lesion, peripheral, BE area, and K^{trans}-mean parameters can contribute to the diagnosis of breast lesions, background enhancement and the pathological grading of malignant tumors.

Background

Breast cancer is the second leading cause of cancer death among women and is the most common malignant tumors in women worldwide [1]. In China, its incidence and mortality are increasing while the age of onset is decreasing [2, 3]. Around 1.6 million people are diagnosed each year and 1.2 million succumb to their illness. Therefore, early and accurate diagnosis is essential to guide the treatment of breast cancer.

Traditional contrast-enhanced magnetic resonance imaging (CE-MRI) plays a central role in the diagnosis of breast pathologies due to its non-invasive and radiation-free nature. Yet, background enhancement (BE) may obscure enhanced lesions or contribute to false-positive readings [4–6]. Routine breast CE-MRI has high sensitivity and low specificity, which limits its diagnostic utility. In view of the heterogeneity of benign and malignant diseases and BE tissues, high-resolution dynamic contrast-enhanced MRI (DCE-MRI) can better evaluate the tissue microenvironment and texture characteristics.

DCE-MRI can predict the biological characteristics of breast cancer, tumor environment, situation [16–18], molecular receptor subtypes [10, 17–20], and even genomics [9, 21, 22]. Quantitative assessment of ROI signal strength, spatial structure and other image parameter characteristics by high-throughput extraction can also offer diagnostic value [7, 8]. For example, the quantitative analysis of the gray level co-occurrence matrix of heterogeneity may be a sign of metastasis and contribute to poor prognosis [9–15]. There is evidence to suggest that factors such as texture evaluation of vasculature, lymphatic permeation, density and angiogenesis are correlated with the prognosis of the disease [26]. Therefore, high-resolution DCE-MRI analysis of texture features can help predict disease prognosis [19, 23–25]. Such utility can help in the early diagnosis of breast cancers [4, 10, 27].

Therefore, in this study, we aimed to investigate the application value of texture analysis based on kinetic parametric maps from breast DCE-MRI for the discrimination of benign lesions, malignant lesions and background parenchymal enhancement using a two-compartment Extended Tofts model and volume of interest.

Methods

Patients

The study was approved by the institutional review board. Written informed consent was obtained. This study prospectively enrolled 128 patients (age range, 23–79 years) with clinically suspected breast disease in our hospital from April 2015 to June 2017. Among them, 62 patients underwent preoperative high temporal resolution DCE-MRI (1 + 26 phases) were collected. 39 malignant lesions (invasive ductal carcinoma, IDC) (age range, 31–77 years; average age, 54.1 years) and 23 benign lesions (age range, 25–79 years; average age, 48.0 years) were confirmed by pathology. 66 patients were either lost to follow up, had no pathological result or had other types of malignant diseases and were excluded. In the control group, 78 patients underwent preoperative low temporal resolution DCE-MRI (1 + 6 phases) were

randomly and retrospectively enrolled, 46 malignant lesions (age range, 32–70 years; average age, 50.0 years) and 32 benign lesions (age range, 23–70 years; average age, 43.5 years) were included. Patients who had undergone neoadjuvant chemotherapy were excluded. The patient flowchart was shown in Fig. 1.

MRI protocol

DCE-MRI examination was performed on a 3.0T MR scanner (Magnetom verio, Siemens Medical Solutions, Erlangen, Germany), equipped with a 16-channel phased-array breast coil. The patient was placed in the prone position with their breasts naturally suspended in the double coil and the head was positioned toward the machine. Routine MRI examination was followed: 3D positioning scan, TIRM (Turbo Inversion Recovery T2-weighted sequence, TIRM) sequence (TR = 4000 ms, TE = 70 ms, Slice thickness = 4 mm, FOV = 34 cm × 34 cm, Matrix = 448 × 448, Nex = 2) with cross-sectional scanning, bilateral sagittal T2-weighted imaging (T2WI, fat suppression) was the following parameters: TR = 4650 ms, TE = 85 ms, Slice thickness = 4 mm, Layer space = 1.0 mm, FOV = 20 cm × 20 cm, Matrix = 320 × 224, Nex = 4).

A high temporal resolution DCE-MRI (1 + 26 phases) scan was conducted with the following parameters: T1 3D Dyna VIEWS, TR = 4.43 ms, TE = 1.38 ms, Slice thickness = 2 mm, FOV = 30 cm × 30 cm, Matrix = 224 × 224, Nex = 1, Flip angle = 15°, Measurement frequency = 27, with a temporal resolution of 11 s and a total scanning time of 5 minutes and 3 seconds. Low temporal resolution DCE MRI (1 + 6 phases) scan was conducted with the following parameters: T1 3D Dyna VIEWS, TR = 4.51 ms, TE = 1.61 ms, Slice thickness = 1 mm, FOV = 34 cm × 34 cm, Matrix = 448 × 448, Nex = 1, Measurement frequency = 6, with a temporal resolution of 60 s, before the contrast injection, immediately after the start of the contrast injection, at 60 s, 120 s, 180 s, 240 s, and 300 s after injection (six acquisitions).

The contrast agent was Gadopentetate dimeglumine (Omniscan, GE Healthcare) at the dosage of 0.1 mmol/kg administered by intravenous bolus injection using a double cylinder high pressure injector (MR injection system) at a flow rate of 2.0 ml/sec,followed by a 10 ml saline flush.

Image analysis

All DCE-MRI image data was transferred into the Omni-Kinetic software (GE Healthcare, version 2.10) to obtain the K^{trans} texture features and the pharmacokinetic parameters ($K^{trans,}$ K_{ep}, V_e and V_p) of the lesion central area (Lesion), surrounding peripheral area (Peri) and background enhancement (BE) area in the malignant and the benign groups using a two-compartment extended Tofts model and three-dimensional volume of interest. All data were analyzed by 2 senior imaging diagnostic radiologists (J.L. with 5 years of experience, and J.Z. with 7 years of experience in breast MRI).

The ROI (region of interest) was manually selected and delineated based on enhanced T1-weighted images and the pharmacokinetic maps. In Fig. 2, a malignant lesion was clearly shown, and a polygon ROI was drawn manually according to the shapes of lesion (lesion area), the surrounding peripheral area

(peri, with a radius of 2.5-5.0 mm depending on pixel size) and background enhancement (BE) area (normal breast background parenchyma enhancement) avoiding the necrotic area and vascular beds.

Hemodynamic parameters included K^{trans} (ml/min, endothelial transfer constant refers to the rate of blood leakage to the extravascular extracellular fluid gap (EES)), K_{ep} (ml/min, reflux rate constant refers to the blood leakage rate from EES back to blood vessels), $V_e = K^{trans}/K_{ep}$ (ml/ml, fractional EES volume refers to the method that fractional EES volume in the EES of the contrast agents), and V_p (ml/ml, fractional plasma volume refers to the plasma volume of contrast agent) was used to quantitatively evaluate the microcirculation characteristics of the lesions.

Texture feature analysis refers to image conversion and quantitative analysis. The image conversion functions to decompose the conventional image into basic components such as space and frequency. Quantitative analysis included the structure, model, statistics and spectrum of various basic components. For each patient, all texture features were obtained based on the K^{trans} map from DCE-MRI images. Texture feature analysis based on high resolution DCE-MRI included the first-order distribution statistics, gray-level co-occurrence matrix (GLCM) and gray-level run-length matrix (GLRLM).

The first-order distribution statistics included energy, skew, maximum, median, mean, mean absolute deviation, range, root mean square, standard deviation, variance, etc. The gray-level histogram is a discrete function of image gray level (formula: $H(i) = ni/N(i = 0, 1,..., L - 1)$, where i represents the grayscale level, L represents the number of grayscale categories, ni represents the number of pixels with grayscale level i in the image, and N represents the total number of pixels in the image), which refers to the probability of occurrence of pixels in the image with grayscale i. GLCM is a statistical method based on the second-order combination condition probability density function to describe texture, local mode, random, and spatial statistical characteristics, and to represent regional consistency and inter-regional relativity. GLRLM is the joint probability density of two position pixels, which reflects the brightness distribution characteristics and the second-order statistical characteristics of the location distribution characteristics between pixels with the same or similar brightness.

Statistical analysis

All statistical analysis was carried out in IBM SPSS Statistics software (version 19.0; BM SPSS, Chicago, 1L, USA), with $P < 0.05$ statistical significance. The Student's *t*-test was used to compare the differences of hemodynamic parameters from high-resolution and low-resolution DCE-MRI of the lesion central area, surrounding peripheral area and background enhancement in the malignant and benign groups (multiple correction by Family-wise error rate). Logistic regression was used to build models based on texture features for the diagnosis of breast lesions and background enhancing efficiency. ROC analysis was used to determine the diagnostic performance of each parameter.

Since the sample size in the benign and malignant groups were not uniform, over-sampling in the smaller group was conducted using the Smote (Synthetic Minority Oversampling Technique) method. For each missing sample in the smaller group, the Euclidean distance was used as the standard to calculate the

distance to all samples in a small sample set, and the nearest neighbor was designated as K. A sampling ratio was set according to the sample imbalance ratio to determine the sampling ratio N. For each minority sample X, a number of samples were randomly selected from its K neighbor, assuming that the selected neighbor was Xn. For each randomly selected nearest neighbor Xn, the new sample was constructed with the original sample respectively according to the following formula:

$$Xnew = X + rand(0, 1) \times (\overline{X} - X)$$

A new sample of high-resolution DCE-MRI group was constructed with the following: 62 cases —>96 cases; a new sample of low resolution DCE-MRI group was constructed with the following: 78 cases —>128 cases.

The samples were randomly divided into the training and testing groups by 0.7:0.3. As the potential correlations among many features easily affect the accuracy of the model, we conducted a three-step dimensionality reduction for the obtained features. In the first step, the single-factor method was used to analyze and select the features with differences; in the second step, the features related to dependent variables were selected through a general linear model; in the third step, feature dimension reduction was used by the LASSO (Least absolute shrinkage and selection operator) method. After dimension reduction, the model was built by logistic regression, and the classification accuracy of the test group was verified. The area under the roc curve (AUC) was calculated. The Delong-test was used to compare the ROC curves of the models.

Results

Study population

There were a total of 62 patients who underwent preoperative high temporal resolution DCE-MRI (1 + 26 phases) scans. 39 malignant lesions (age range, 31–77 years; average age, 54.1 years; 17 cases located in the right breast, 22 cases located in the left) and 23 benign lesions (age range, 25–79 years; average age, 48.0 years) were identified. In the control group, 78 patients underwent preoperative low temporal resolution DCE-MRI (1 + 6 phases) scans, which demonstrated 46 malignant (age range, 32–70 years; average age, 50.0 years; 21 cases located in the right breast, 25 cases located in the left) and 32 benign lesions (age range, 23–70 years; average age, 43.5 years). Table 1 showed general characteristics in this study.

Table 1
The general characteristics of this study

Characteristics	High-temporal resolution DCE-MRI		Low- temporal resolution DCE-MRI	
	Malignant	Benign	Malignant	Benign
Number	39	23	46	32
Age (years)				
Median (range)	53 (31–77)	48 (25–79)	49 (32–70)	48 (23–70)
Mean ± Standard	54.1 ± 11.4	48.0 ± 11.4	50.0 ± 9.0	43.5 ± 10.5
Pathology grade				
Grade I	5	N	5	N
Grade II	16	N	15	N
Grade III	18	N	26	N

Note: N means None.

Hemodynamic parameters obtained from DCE-MRI compared in benign and malignant groups

The hemodynamic characteristics obtained from high-temporal resolution DCE-MRI and low temporal resolution DCE-MRI were compared in the benign and malignant groups. It was found that there was a statistical difference ($P < 0.05$, corrected by FWE). According to Table 2**(a, b)**, there were significant differences in the values of K^{trans}, K_{ep}, V_e, V_p and TTP between the two DCE-MRI groups in the lesion central area, surrounding peripheral area, and background enhancement area ($p < 0.05$). The results indicated that the hemodynamic parameters obtained from two different temporal resolutions had a statistically significant difference.

Table 2 A

Hemodynamic parameters obtained from DCE-MRI compared to the malignant group

Hemodynamic parameters	Lesion Area (*P* value)	Peri area (*P* value)	BE area (*P* value)
K^{trans} Mean	1.83347E-10	1.47E-16	1.07E-13
K^{trans} Standard	1.30519E-22	1.52E-31	1.84E-23
K_{ep} Mean	2.98583E-13	0.002676	0.031604
K_{ep} Standard	0.005468862	0.018207	1.77E-09
V_e Mean	0.00330491	0.730905	1.15E-10
V_e Standard	2.12427E-31	4.66E-24	2.28E-26
V_p Mean	6.17281E-29	4.46E-25	6.97E-24
V_p Standard	1.75369E-32	1.72E-46	1.99E-41
TTP Mean	0.009275042	1.16E-12	5.28E-07
TTP Standard	0.044384646	0.053585	0.1607

Note: Lesion=Breast lesion central area, Peri=Surrounding peripheral lesion area, BE=Background parenchyma enhancement area; Multi-correction using Family-wise-error.

Table 2 B
Hemodynamic parameters obtained from DCE-MRI compared in the benign group

Hemodynamic parameters	Lesion area (*P* value)	Peri area (*P* value)	BE area (*P* value)
K^{trans} Mean	1.1265E-08	2.6789E-09	6.91583E-11
K^{trans} Standard	2.04163E-14	6.92625E-17	4.54596E-09
K_{ep} Mean	0.000339134	0.273137134	0.57822515
K_{ep} Standard	0.036088902	0.003251275	0.067364479
V_e Mean	0.164739849	0.401025528	8.89586E-08
V_e Standard	1.95556E-16	1.13582E-14	1.44275E-07
V_p Mean	1.45352E-17	1.15098E-17	3.78791E-15
V_p Standard	1.03139E-10	2.21574E-28	3.94651E-08
TTP Mean	3.03667E-05	2.04714E-06	1.19164E-06
TTP Standard	0.43272682	0.606416866	0.341144857

Note: Lesion=Breast lesion central area, Peri=Surrounding peripheral lesion area, BE=Background parenchyma enhancement area; Multi-correction using Family-wise-error.

In the malignant group, the correlation between hemodynamic parameters and pathological grade (Grade I to III) of invasive ductal carcinoma (IDC) was further analyzed. It was found that the lesion K^{trans}- mean of the high-temporal resolution DCE-MRI group was significantly correlated to the pathological grading (r = 0.400, P = 0.012). In contrast, the low-temporal resolution DCE-MRI group had no correlation with the pathological grade (r = − 0,012, P > 0.05).

Performance of K^{trans} texture feature models based on two temporal resolution DCE-MRI

According to the classification model constructed of the texture features based on K^{trans} map from DCE-MRI, the AUC, accuracy, sensitivity and specificity of models from the high-temporal resolution DCE-MRI (1 + 26 phases) group were higher than those of the low-temporal resolution DCE-MRI (1 + 5 phases) group (Table 3, Fig. 3).

Table 3

ROC curves of K^{trans} texture feature models from the high- and low-resolution DCE-MRI for breast malignant and benign lesions

ROI	AUC	95% Confidence Interval	ACC	SPC	SEN
High-resolution DCE-MRI group					
Lesion	0.889	0.759-1.000	0.867	0.933	0.867
Peri	0.884	0.734-1.000	0.733	0.933	0.867
BE	0.760	0.575–0.945	0.700	0.867	0.667
Lesion + Peri + BE	0.933	0.852-1.000	0.800	0.933	0.800
Low-resolution DCE-MRI group					
Lesion	0.850	0.725–0.975	0.750	0.800	0.800
Peri	0.835	0.703–0.967	0.725	0.750	0.850
BPE	0.716	0.518–0.913	0.733	0.800	0.667
Lesion + Peri + BE	0.868	0.723-1.000	0.833	0.786	0.900

Note: ROI=Region of interest, Lesion=Breast lesion central area, Peri=Surrounding peripheral lesion area, BE=Background parenchyma enhancement area, AUC=Area under the curve, ACC=Accuracy, SPC=Specificity, SEN= Sensitivity

ROC curves showed that the models based on the K^{trans} texture features obtained from high-temporal resolution DCE-MRI for benign and malignant lesions had the following values for the AUC, accuracy, sensitivity, and specificity, respectively. For the central area, 0.889, 0.867, 0.867, and 0.933; for the surrounding peripheral area, 0.884, 0.733, 0.867, and 0.933; for the background enhancement, 0.760, 0.700, 0.667, and 0.867; for the (Lesion + Peri + BE) area 0.933, 0.800, 0.800, and 0.933.

ROC curves showed that the models based on the K^{trans} texture features obtained from low-temporal resolution DCE-MRI for benign and malignant lesions had the following values for the AUC, accuracy, sensitivity, and specificity, respectively. For the central area, 0.850, 0.750, 0.800 and 0.800; for the surrounding peripheral area 0.835, 0.725, 0.850, and 0.750; for the background enhancement, 0.716, 0.733, 0.667, and 0.800 respectively; for the (Lesion + Peri + BE) area, 0.868, 0.833, 0.900, and 0.786.

After using the Delong-test to evaluate models between the two DCE-MRI groups, there was no significant difference ($P > 0.05$). The reason may be due to a small sample size. These results indicated that high-temporal resolution DCE-MRI had more diagnostic value in the diagnosis of breast disease and background enhancement. The K^{trans} texture features of the lesion, peripheral and background enhancement area may be helpful for the differentiation of benign and malignant lesions, particularly when combining three areas.

Discussion

In this study, we conducted a randomized controlled study on preoperative high-temporal resolution and low-temporal resolution DCE-MRI texture features, including the lesion central area, surrounding peripheral area, and background enhancement area. The quantitative parameters were measured by volume measurement, and the ROI area was selected to be larger, which was more comprehensive and accurate than the data measured at a single level in most previous studies. Neoadjuvant chemotherapy patients were excluded to avoid the effect of therapy on lesions. These results in this study indicated that high-temporal resolution DCE-MRI may be more helpful than low-temporal resolution DCE-MRI in the differentiation of breast disease from background enhancement.

Most previous studies have focused only on the disease itself [8–18, 21, 22] or the peripheral interstitial areas [19, 23, 24]. The lesion center, periphery and background enhancement area may be related to the differentiation of benign and malignant lesions. Few studies have comprehensively focused on the aforementioned area by volume measurement. The region of interest in this study included the lesion central area, surrounding peripheral area and background enhancement area. Therefore, the data were as comprehensive. It was found that the three ROI's hemodynamic characteristics (K^{trans}, K_{ep}, V_e, V_p, TTP) obtained from two different temporal resolution DCE-MRI had a statistical difference. Particularly, the joint K^{trans} texture features of three areas may be helpful for the differentiation of benign and malignant breast disease. These results indicated that the comprehensive measurement of lesions and background enhancement area could be more accurate in the diagnosis and differentiation of benign and malignant lesions.

In this study, the ROC curve showed that models from the high-temporal resolution DCE-MRI group were slightly higher than those of the low-temporal resolution DCE-MRI group, which meant that DCE-MRI with high temporal resolution had high application value in the diagnosis of breast diseases. Conventional breast dynamic enhanced MRI mainly observed the characteristic of time signal intensity curve of breast disease (i.e curve shape, time to peak, early enhancement rate, etc.) and allowed for semiquantitative analysis of tumor characters. But these semiquantitative parameters were influenced by the cardiac output, imaging sequences, contrast medium injection rate, blood flow and so on, which were prone to error [30]. This study used quantitative analysis based on breast DCE - MRI by the Extended Tofts model and obtained multiple hemodynamic parameters, such as the endothelial transfer constant of K^{trans}, reflux rate of K_{ep}, fractional EES volume of V_e and fractional plasma volume of V_p. The extended Tofts model was applicable to the time resolution of < 12 seconds, as high temporal resolution can more accurately measure the lesion and observe subtle pharmacokinetic changes in tissue for a very short time. This allows the sequence to accurately capture characters of the lesion, even including subtle differences of contrast agent concentration changes. Thus, high-temporal resolution may extract more texture features than low-temporal resolution for accurate diagnosis of breast lesions [31, 32].

Although pathology is the gold standard for disease analysis and classification, it is limited by invasiveness and local sampling, which may cause inaccurate pathological results and the limited

pathological classification of diseases. DCE-MRI has become an important method of diagnosis and observation of breast diseases due to its noninvasive, radiation-free and high-resolution nature with soft tissue. In this study, we analyzed the correlation between DCE-MRI and pathological grading of malignant lesions (invasive ductal carcinoma, IDC). The results showed that only the K^{trans}-mean of lesion central area on the high-temporal resolution DCE-MRI was significantly correlated with pathological grade [33]. In this study, invasive ductal carcinoma was only included in the malignant group because the number of patients with other malignant types was too small (less than 5 cases) to be excluded by correlation statistics of pathological grade. These indicated that high-temporal resolution DCE-MRI may offer more diagnostic information in a lesion.

It was determined that K^{trans}-mean reflects the hemodynamic characteristics of the disease and was related to the number and immaturity degree of blood vessels in the central tumor and peritumor regions in different pathological grades. Tumor angiogenesis increased in most malignant lesions, and there were a large number of immature tumors with high permeability of their vessel walls. Therefore, low molecular weight contrast agents were able to enter the EES through the thin vessel walls. Some previous studies also support that high-temporal resolution DCE-MRI can more accurately evaluate the hemodynamic microenvironment of tissues, through high-throughput extracted image texture features and quantitative evaluation. For example, the gray level co-occurrence matrix with the quantitative enhancement of heterogeneity can predict breast cancer invasion, prognosis and curative effect [7, 9–15].

Interestingly, this study found that the performance of K^{trans} texture feature models of lesion, peripheral and background enhancement area based on high-temporal resolution DCE-MRI had more slightly high than low resolution, particularly joint textural feature model of three areas better than others. Background enhancement (BE) of the breast reflects an increase of T1 relaxation after enhancement, which directly reflects the blood supply and permeability of breast tissue. Hormones, especially estrogen, increase the microvascular permeability and vasodilation of breast tissue, causing vascular hyperplasia and ductal gland epithelial proliferation. Progesterone increases metabolic activity by promoting mitosis and leads to increased perfusion of the breast tissue, resulting in background enhancement of the breast. Tissue enhancement in MR imaging is related to vascular distribution, the permeability of contrast agents and T1 relaxation of the tissue [28]. In breast tissue, the anatomy of the vascular system and the effect of hormones on breast tissue are factors affecting the morphology and degree of BE [29]. High resolution dynamic enhanced MR texture can quantitatively evaluate disease and tissue heterogeneity, which is helpful for accurate assessment and early diagnosis of breast diseases and BE [4, 10, 27]. Thus, not only can high-temporal resolution DCE-MRI provide a high application value in the diagnosis of breast disease and background enhancement, but also allows for joint texture features of the lesion.

There were several limitations in this study: First, the sample size was relatively small. When the number of texture features to be extracted and screened was large, the sample size was challenged, which needs further study with large samples. Second, malignant breast lesions of other pathological types of the breast were not included in the group, which needs to be further studied. Third, high time resolution DCE-MRI scan still needs to be further improved to further optimize the scanning time. Fourth, the textural

features model in this study was not further outside this center. Therefore, a multi-center validation can be implemented and add clinical characteristics to the model in the future.

Conclusions

In summary, quantitative analysis with high temporal resolution DCE-MRI has slightly high application value in the diagnosis of breast lesions and background enhancement. The joint texture analysis of the lesion, peripheral area and BE area based on high temporal resolution DCE-MRI may more helpful in the diagnosis, and the K^{trans}-mean parameter may contribute to the pathological grading of malignant tumors. Thus, the use of texture analysis based on high temporal resolution DCE-MRI may potentially improve breast cancer diagnostic performance.

Abbreviations

DCE-MRI
Dynamic contrast-enhanced magnetic resonance imaging
K^{trans}
Endothelial transfer constant
K_{ep}
Reflux rate constant
EES
Extravascular extracellular space
V_e
Fractional EES volume
V_p
Fractional plasma volume
AUC
Area under curve
ROC
Receiver operating characteristic
ROI
Region of interest

Declarations

Ethics approval and consent to participate:

All procedures performed in studies involving human participants were in accordance with the ethical standards of the institutional and/or national research committee and with the 1964 Helsinki declaration and its later amendments or comparable ethical standards.

The Ethics Committee of the First Affiliated Hospital of Zhejiang Chinese Medical University has approved this study, in which informed consent was written, and patient confidentiality was protected.

Consent for publication

Not applicable

Availability of data and materials:

The data that support the findings of this study are available from the corresponding author upon reasonable request.

Competing interests:

The authors declare that they have no competing of interests.

Funding:

This study was supported by Zhejiang Traditional Chinese Medicine Science and Technology Project (2018ZB048), Zhejiang Provincial Department of Health Platform Backbone Project (2016147237), Medical Health Science and Technology Project of Zhejiang Provincial Health Commission (2020KY199, WKJ-ZJ-2039). The funders had roles in the design of the study, data collection, analysis, and in manuscript writing.

Authors' Contributions:

All authors contributed to this paper. YL and JL: Writing original draft, Data curation, Data analysis. JQ: Data curation, Data analysis, Visualization. RT: Software, Data analysis, Visualization. KL: Software, Validation, Visualization. CW: Data Curation, Data analysis. FX: Data Curation, Data analysis. JZ: Data curation. MG: Data curation. XD: Data Curation. HD: Data Curation. MX and SW: Conceptualization, Methodology, Supervision, Project administration, Writing review and editing. All authors read and approved the final manuscript.

Acknowledgements:

The authors thank all the medical staff who contributed to the maintenance of the medical record database.

References

1. Torre LA, Trabert B, DeSantis CE, et al. Ovarian cancer statistics, 2018. CA Cancer J Clin. 2018;68(4):284–96. doi:10.3322/caac.21456.
2. Fan L, Strasser-Weippl K, Li JJ, et al. Breast cancer in China. Lancet Oncol. 2014;15(7):e279–89. doi:10.1016/S1470-2045(13)70567-9.

3. Goss PE, Strasser-Weippl K, Lee-Bychkovsky BL, et al. Challenges to effective cancer control in China, India, and Russia. Lancet Oncol. 2014;15(5):489–538. doi:10.1016/S1470-2045(14)70029-4.
4. Arasu VA, Miglioretti DL, Sprague BL, et al. Population-Based Assessment of the Association Between Magnetic Resonance Imaging Background Parenchymal Enhancement and Future Primary Breast Cancer Risk. J Clin Oncol. 2019;37(12):954–63. doi:10.1200/JCO.18.00378.
5. Scaranelo AM, Carrillo MC, Fleming R, Jacks LM, Kulkarni SR, Crystal P. Pilot study of quantitative analysis of background enhancement on breast MR images: association with menstrual cycle and mammographic breast density. Radiology. 2013;267(3):692–700. doi:10.1148/radiol.13120121.
6. Klifa C, Suzuki S, Aliu S, et al. Quantification of background enhancement in breast magnetic resonance imaging. J Magn Reson Imaging. 2011;33(5):1229–34. doi:10.1002/jmri.22545.
7. Giess CS, Raza S, Birdwell RL. Patterns of nonmasslike enhancement at screening breast MR imaging of high-risk premenopausal women. Radiographics. 2013;33(5):1343–60. doi:10.1148/rg.335125185.
8. Forghani R, Srinivasan A, Forghani B. Advanced Tissue Characterization and Texture Analysis Using Dual-Energy Computed Tomography: Horizons and Emerging Applications. Neuroimaging Clin N Am. 2017;27(3):533–46. doi:10.1016/j.nic.2017.04.007.
9. Zhu Y, Li H, Guo W, et al. Deciphering Genomic Underpinnings of Quantitative MRI-based Radiomic Phenotypes of Invasive Breast Carcinoma. Sci Rep. 2015;5:17787. doi:10.1038/srep17787.
10. Agner SC, Rosen MA, Englander S, et al. Computerized image analysis for identifying triple-negative breast cancers and differentiating them from other molecular subtypes of breast cancer on dynamic contrast-enhanced MR images: a feasibility study. Radiology. 2014;272(1):91–9. doi:10.1148/radiol.14121031.
11. Ashraf A, Gaonkar B, Mies C, et al. Breast DCE-MRI Kinetic Heterogeneity Tumor Markers: Preliminary Associations with Neoadjuvant Chemotherapy Response. Transl Oncol. 2015;8(3):154–62. doi:10.1016/j.tranon.2015.03.005.
12. Burnside ES, Drukker K, Li H, et al. Using computer-extracted image phenotypes from tumors on breast magnetic resonance imaging to predict breast cancer pathologic stage. Cancer. 2016;122(5):748–57. doi:10.1002/cncr.29791.
13. Fan M, Zhang P, Wang Y, et al. Radiomic analysis of imaging heterogeneity in tumours and the surrounding parenchyma based on unsupervised decomposition of DCE-MRI for predicting molecular subtypes of breast cancer. Eur Radiol. 2019;29(8):4456–67. doi:10.1007/s00330-018-5891-3.
14. Kim JH, Ko ES, Lim Y, et al. Breast Cancer Heterogeneity: MR Imaging Texture Analysis and Survival Outcomes. Radiology. 2017;282(3):665–75. doi:10.1148/radiol.2016160261.
15. Wu J, Gong G, Cui Y, Li R. Intratumor partitioning and texture analysis of dynamic contrast-enhanced (DCE)-MRI identifies relevant tumor subregions to predict pathological response of breast cancer to neoadjuvant chemotherapy. J Magn Reson Imaging. 2016;44(5):1107–15. doi:10.1002/jmri.25279.
16. Guo W, Li H, Zhu Y, et al. Prediction of clinical phenotypes in invasive breast carcinomas from the integration of radiomics and genomics data. J Med Imaging (Bellingham). 2015;2(4):041007.

doi:10.1117/1.JMI.2.4.041007.

17. Li H, Zhu Y, Burnside ES, et al. Quantitative MRI radiomics in the prediction of molecular classifications of breast cancer subtypes in the TCGA/TCIA data set. NPJ Breast Cancer. 2016;2:16012-. doi:10.1038/npjbcancer.2016.12.
18. Waugh SA, Purdie CA, Jordan LB, et al. Magnetic resonance imaging texture analysis classification of primary breast cancer. Eur Radiol. 2016;26(2):322–30. doi:10.1007/s00330-015-3845-6.
19. Nagasaka K, Satake H, Ishigaki S, Kawai H, Naganawa S. Histogram analysis of quantitative pharmacokinetic parameters on DCE-MRI: correlations with prognostic factors and molecular subtypes in breast cancer. Breast Cancer. 2019;26(1):113–24. doi:10.1007/s12282-018-0899-8.
20. Sutton EJ, Dashevsky BZ, Oh JH, et al. Breast cancer molecular subtype classifier that incorporates MRI features. J Magn Reson Imaging. 2016;44(1):122–9. doi:10.1002/jmri.25119.
21. Wan T, Bloch BN, Plecha D, et al. A Radio-genomics Approach for Identifying High Risk Estrogen Receptor-positive Breast Cancers on DCE-MRI: Preliminary Results in Predicting OncotypeDX Risk Scores. Sci Rep. 2016;6:21394. doi:10.1038/srep21394.
22. Li H, Zhu Y, Burnside ES, et al. MR Imaging Radiomics Signatures for Predicting the Risk of Breast Cancer Recurrence as Given by Research Versions of MammaPrint, Oncotype DX, and PAM50 Gene Assays. Radiology. 2016;281(2):382–91. doi:10.1148/radiol.2016152110.
23. Keller BM, Chen J, Conant EF, Kontos D. Breast density and parenchymal texture measures as potential risk factors for Estrogen-Receptor positive breast cancer. Proc SPIE Int Soc Opt Eng. 2014;9035:90351D. doi:10.1117/12.2043710.
24. Wu S, Weinstein SP, DeLeo MJ 3rd, et al. Quantitative assessment of background parenchymal enhancement in breast MRI predicts response to risk-reducing salpingo-oophorectomy: preliminary evaluation in a cohort of BRCA1/2 mutation carriers [published correction appears in Breast Cancer Res. 2015;17:144]. Breast Cancer Res. 2015;17:67. doi:10.1186/s13058-015-0577-0.
25. Wu S, Berg WA, Zuley ML, et al. Breast MRI contrast enhancement kinetics of normal parenchyma correlate with presence of breast cancer. Breast Cancer Res. 2016;18(1):76. doi:10.1186/s13058-016-0734-0.
26. Ocaña A, Diez-Gónzález L, Adrover E, Fernández-Aramburo A, Pandiella A, Amir E. Tumor-infiltrating lymphocytes in breast cancer: ready for prime time? J Clin Oncol. 2015;33(11):1298–9. doi:10.1200/JCO.2014.59.7286.
27. Wang TC, Huang YH, Huang CS, et al. Computer-aided diagnosis of breast DCE-MRI using pharmacokinetic model and 3-D morphology analysis. Magn Reson Imaging. 2014;32(3):197–205. doi:10.1016/j.mri.2013.12.002.
28. Winfield JM, Payne GS, deSouza NM. Functional MRI and CT biomarkers in oncology. Eur J Nucl Med Mol Imaging. 2015;42(4):562–78. doi:10.1007/s00259-014-2979-0.
29. Giess CS, Yeh ED, Raza S, Birdwell RL. Background parenchymal enhancement at breast MR imaging: normal patterns, diagnostic challenges, and potential for false-positive and false-negative interpretation. Radiographics. 2014;34(1):234–47. doi:10.1148/rg.341135034.

30. Georgiou L, Wilson DJ, Sharma N, Perren TJ, Buckley DL. A functional form for a representative individual arterial input function measured from a population using high temporal resolution DCE MRI. Magn Reson Med. 2019;81(3):1955–63. doi:10.1002/mrm.27524.
31. Cheng Z, Wu Z, Shi G, et al. Discrimination between benign and malignant breast lesions using volumetric quantitative dynamic contrast-enhanced MR imaging. Eur Radiol. 2018;28(3):982–91. doi:10.1007/s00330-017-5050-2.
32. Jena A, Taneja S, Singh A, Negi P, Mehta SB, Sarin R. Role of pharmacokinetic parameters derived with high temporal resolution DCE MRI using simultaneous PET/MRI system in breast cancer: A feasibility study. Eur J Radiol. 2017;86:261–6. doi:10.1016/j.ejrad.2016.11.029.
33. Pinker K, Helbich TH, Morris EA. The potential of multiparametric MRI of the breast [published correction appears in Br J Radiol. 2017 Apr;90(1072):20160715e]. Br J Radiol. 2017;90(1069):20160715. doi:10.1259/bjr.20160715.

Figures

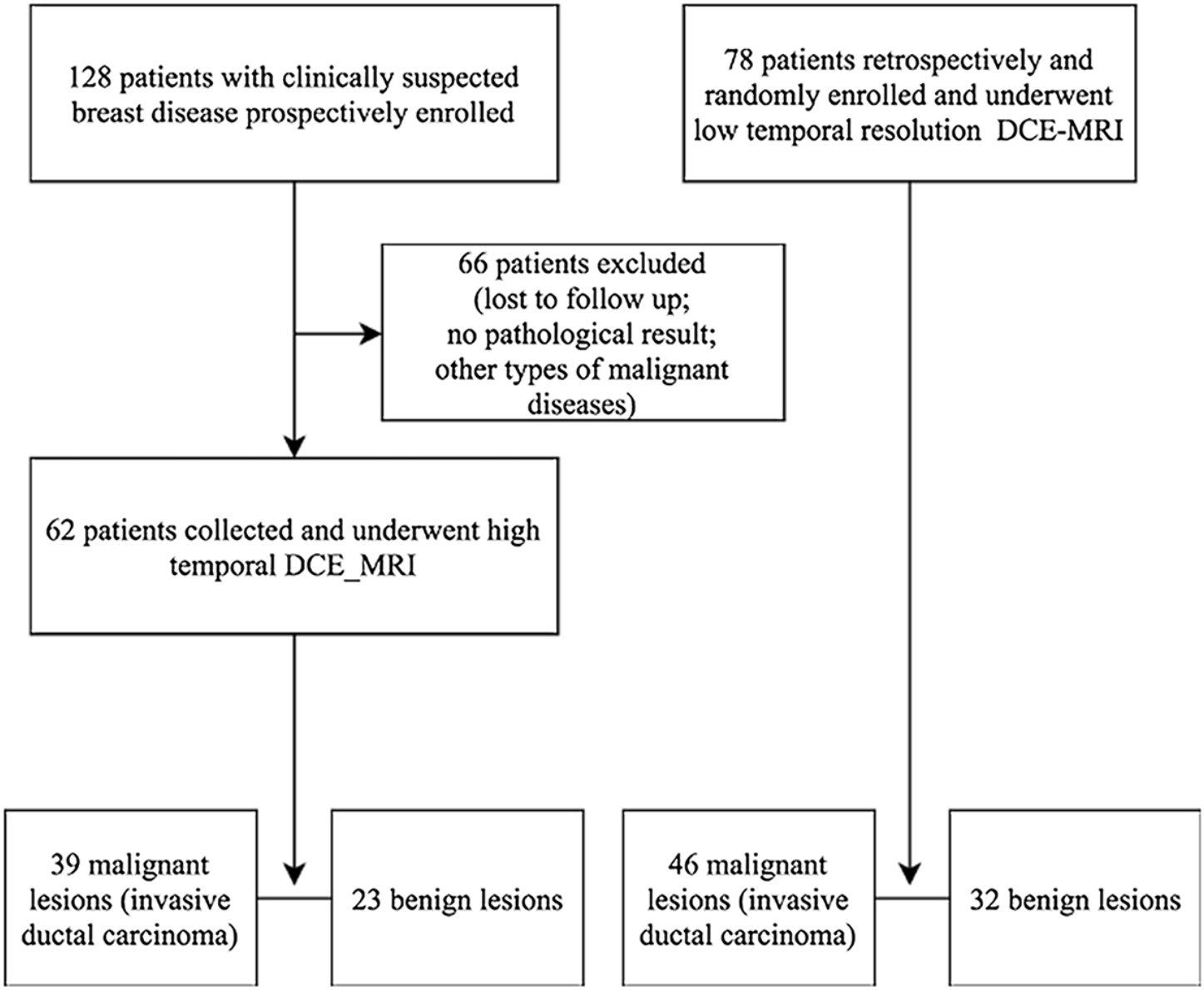

Figure 1

The patient inclusion flowchart was shown.

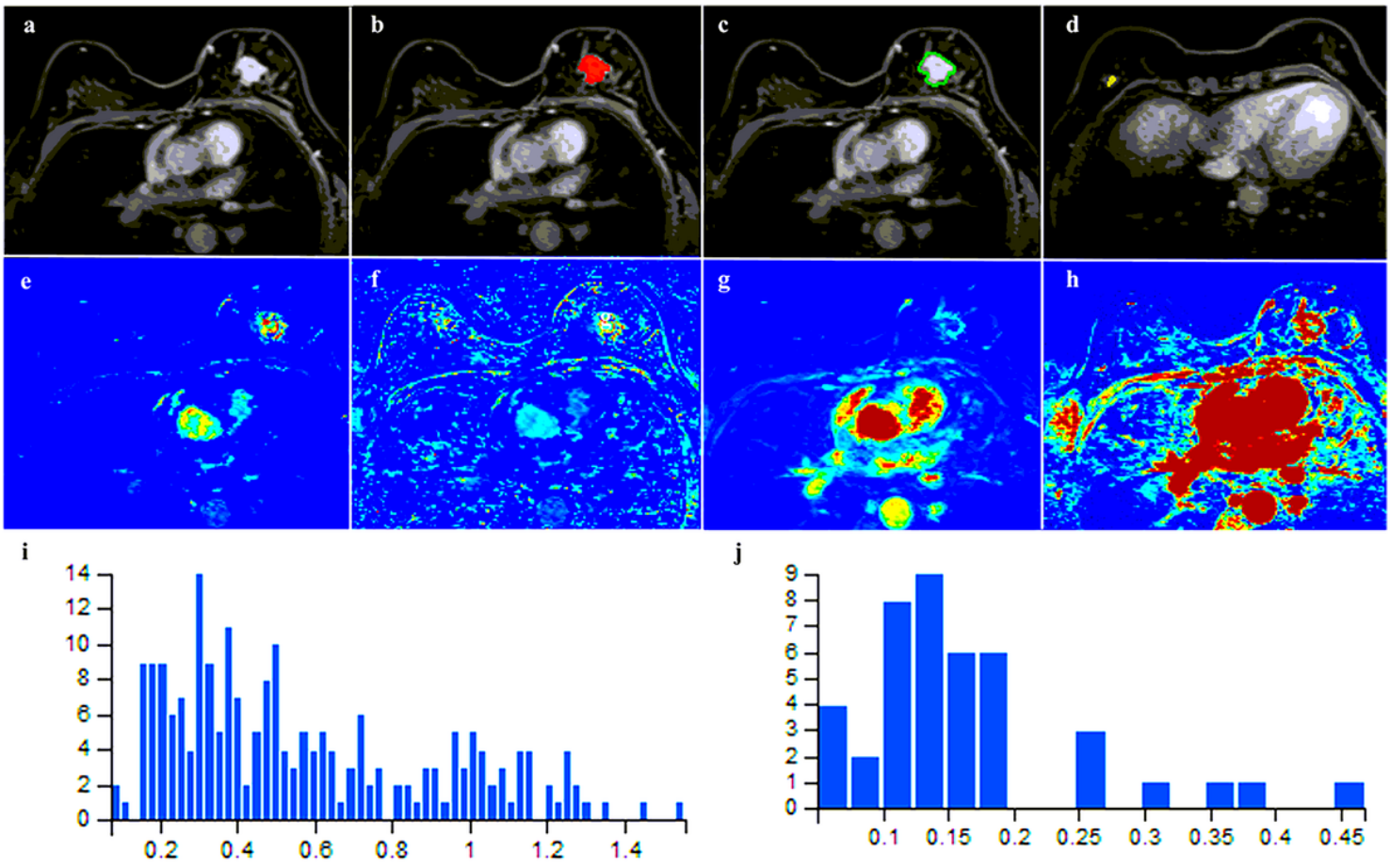

Figure 2

A malignant lesion was clearly identified on enhanced T1-weighted imaging (a-d), Kep (e), Vp (f), Ktrans (g) and Ktrans-map (h) from the high temporal resolution DCE-MRI. The histogram of texture features was also obtained from the central lesion area (i) and normal area (j). All ROIs were drawn manually according to the shape of the lesion (b), the surrounding peripheral area (c) and background enhancement (d) while avoiding the necrotic area and vascular beds

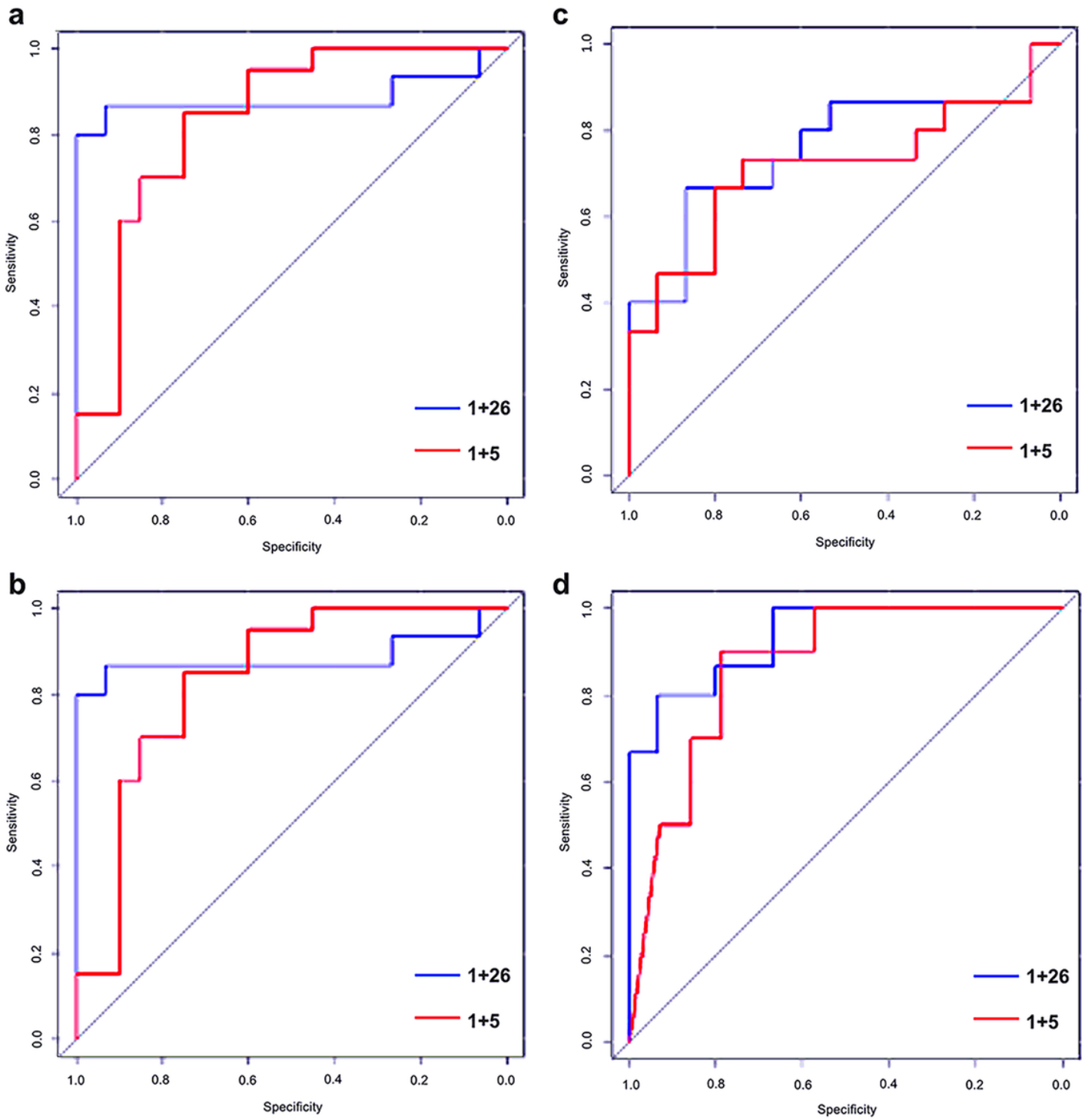

Figure 3

(a-d) ROC curve of the Ktrans texture features model from high-temporal resolution DCE-MRI (1+26 phases) (blue line) and low-temporal resolution DCE-MRI (1+6 phases) DCE-MRI (red line) in the lesion central area (Lesion, a), surrounding peripheral area (Peri, b), background enhancement (BE, c) area, and (Lesion + Peri + BE, d) area. (a) AUC values of two lesion area models were 0.889 and 0.850 respectively; (b) AUC values of two Peri area models were 0.884 and 0.835 respectively; (c) AUC values of two BE area

models were 0.76 and 0.716 respectively; (d) AUC values of two (Lesion+Peri+BE) area models were 0.933 and 0.868 respectively.